Available online at www.sciencedirect.com

SciVerse ScienceDirect

Ceramics International 38 (2012) 3563–3567

CERAMICS INTERNATIONAL

www.elsevier.com/locate/ceramint

Fabrication and CO gas-sensing properties of Pt-functionalized Ga_2O_3 nanowires

Hyunsu Kim, Changhyun Jin, Soyeon An, Chongmu Lee *

Department of Materials Science and Engineering, Inha University, 253 Yonghyun-dong, Incheon 402-751, Republic of Korea

Received 12 December 2011; received in revised form 23 December 2011; accepted 27 December 2011
Available online 2 January 2012

Abstract

Ga_2O_3 one-dimensional (1D) nanostructures were synthesized using an evaporation technique. The morphology, crystal structure and enhanced sensing properties of the Ga_2O_3 nanostructures functionalized with Pt to CO gas at 100 °C were examined. The diameter and lengths of the 1D nanostructures ranged from a few tens to a few hundreds of nanometers and up to a few hundreds of micrometers, respectively. Pt nanoparticles with diameters of a few tens of nanometers were distributed over the Ga_2O_3 nanowires. Multiple networked gas sensors fabricated from these Pt-functionalized Ga_2O_3 nanowires exhibited enhanced electrical responses to CO gas. The responses of the nanowires were improved 27.8, 26.1, 22.0 and 16.9 fold at CO concentrations of 10, 25, 50, and 100 ppm, respectively, Compared to the bare Ga_2O_3 nanowires. The mechanism responsible for the enhanced gas sensing properties of the Pt-functionalized Ga_2O_3 nanowires is discussed.

Keywords: Gas sensor; Pt-functionalized; Ga_2O_3 nanowires; CO gas

1. Introduction

Monoclinic gallium oxide (β-Ga_2O_3) is an important wide band gap semiconductor material with potential applications as high temperature gas sensors [1–4], transparent conducting electrodes [5], phosphors [6] and dielectric gates [7]. Recent studies of Ga_2O_3 thin film-based gas sensors reported the efficient detection of O_2, H_2, CO and CH_4 gases at high temperatures (600–1000 °C) [8,9]. On the other hand, they showed very poor performance at room temperature, which has limited the practical use of Ga_2O_3-based gas sensors.

One-dimensional (1D) nanostructure-based sensors have attracted considerable interest owing to their higher sensitivity, superior spatial resolution and rapid response associated with individual 1D nanostructures due to the high surface-to-volume ratios compared to thin film gas sensors [10–14]. On the other hand, improving their sensing performance and detection limit is still a challenge. A range of techniques, such as doping [15–17], surface functionalization [15,18,19], and fabrication of heterostructures [20–22], have been developed to improve the sensitivity, stability, response and recovery speed of 1D nanostructure-based sensors. Among these, functionalization of the nanowire surfaces with a catalyst, such as Pd and Pt, may be the simplest and most effective technique because the resistance of the sensor changes significantly upon exposure to a target gas at room temperature. The optical and electrical properties of 1D nanostructures coated with a catalyst can change upon exposure to a gas and can be restored upon re-exposure to air, even at room temperature [23–30]. Such low temperature-processes are desirable for the safe detection of toxic gases. Ga_2O_3 1D nanostructure-based sensors, however, still have the same problems as Ga_2O_3 thin film-based gas sensors; high working temperature. This paper reports the synthesis of Ga_2O_3 nanowires by thermal evaporation as well as the enhanced sensing properties of Pt-functionalized Ga_2O_3 nanowires for the detection of CO gas at 100 °C.

2. Experimental

Au-coated Si was used as a substrate for the synthesis of 1D β-Ga_2O_3 structures. Au was initially deposited on a (1 0 0) Si substrate by radio frequency magnetron sputtering. A quartz tube was mounted horizontally inside a tube furnace. GaN powders (99.99% purity) were placed on the lower holder at the

* Corresponding author. Tel.: +82 32 860 7536; fax: +82 32 862 5546.
E-mail address: cmlee@inha.ac.kr (C. Lee).

0272-8842/$36.00
doi:10.1016/j.ceramint.2011.12.072

center of the quartz tube. An Au-coated Si substrate was placed on the upper holder, approximately 5 mm away from the GaN powders. The furnace was heated to 1050 °C and maintained at that temperature for 1 h in a N_2/3 mol%-O_2 atmosphere at constant flow rates of O_2 (15 sccm) and N_2 (485 sccm). The total pressure was set to 1.5 Torr.

A thin Pt film was deposited on the surfaces of some of the as-synthesized β-Ga_2O_3 nanowire samples by direct current (dc) magnetron sputtering (substrate temperature: room temperature, current: 20 mA, working pressure: 1.9×10^{-2} Torr, and process time: 180 s). The Pt-coated nanowires were annealed at 800 °C for 30 min in an Ar atmosphere. The Ar gas flow rate and process pressure were 100 standard cubic centimeters per minute (sccm) and 0.8 Torr, respectively. The nanowire samples were characterized by scanning electron microscopy (SEM, Hitachi S-4200), transmission electron microscopy (TEM, Philips CM-200). The chemical composition was determined by equipped with an energy dispersive X-ray spectroscopy (EDS) attached to the transmission electron microscope.

The as-grown Pt-functionalized Ga_2O_3 nanowires were dispersed by ultrasonication in a mixture of deionized water (5 ml) and isopropyl alcohol (5 ml). A 200 nm thick SiO_2 film was grown thermally on a single crystalline Si (1 0 0) substrate. A slurry droplet containing Ga_2O_3 nanowires (10 μl) was dropped onto the SiO_2-coated Si substrates equipped with a pair of interdigitated (IDE) Ni (∼200 nm)/Au (∼50 nm) electrodes with a gap of 20 μm. The gas sensing properties of the as-synthesized and Pt-functionalized Ga_2O_3 nanowires were measured at 100 °C in a quartz tube inserted in an electric furnace. A given amount of CO (>99.99%) gas was injected into the testing tube through a microsyringe to obtain CO concentrations of 10, 25, 50, or 100 ppm. At the same time, the electrical resistance of the nanowires was monitored. The electrical resistance of the gas sensors was determined by measuring the electric current flowing when a potential difference of 0.5 V was applied between the IDE Ni/Au electrodes. The response of the n-type Ga_2O_3 nanowire sensors was defined as $(R_a - R_g)/R_g$ for a reducing gas, CO, where R_a and R_g are the electrical resistances of sensors in air and target gas, respectively. The response time was defined as the time required for the variation in electrical resistance to reach 90% of the equilibrium value after injecting the gas, and the recovery time was defined as the time needed for the sensor to return to 90% above the original resistance in air after removing the gas.

3. Results and discussion

Fig. 1a shows a typical SEM image of the β-Ga_2O_3 1D nanostructures synthesized on the Si (1 0 0) substrate using a thermal evaporation technique. The diameters of the 1D nanostructures ranged from a few tens to a few hundreds of nanometers and the lengths were up to a few hundreds of micrometers. EDS (Fig. 1b) of a typical Pt-coated Ga_2O_3 nanowire (Fig. 1a, inset) revealed the presence of Ga, Pt, Cu and O. The Cu in the spectra was attributed to the TEM grid. Fig. 1c shows the XRD patterns of the Pt-coated β-Ga_2O_3 nanowires. Most of the peaks in the pattern from the nanowire sample were assigned to β-Ga_2O_3 with a monoclinic structure, but two extra peaks characteristic of metal Pt, which are marked by red dots (JCPDS No. 04-0802, $a = 0.39$ nm), were also identified and indexed to the (1 1 1) and (2 0 0) planes from Pt.

The low-magnification TEM image (Fig. 1d) showed that Pt nanoparticles with diameters of a few tens of nanometers were distributed uniformly around a Ga_2O_3 nanowire. The local high-resolution TEM (HRTEM) image (Fig. 1e) exhibited clear fringe patterns, indicating that both Ga_2O_3 nanowires and Pt nanoparticles are monocrystalline. The resolved distance between the two neighboring parallel fringes in the Ga_2O_3 nanowires region was 0.29 nm, which is in good agreement with the interplanar spacing of the (4 0 0) planes in β-Ga_2O_3. The resolved distance between two neighboring parallel fringes in a Pt nanoparticle was 0.22 nm. This is in good agreement with the interplanar spacing of the (1 1 1) planes in face-centered cubic (fcc)-structured Pt. The corresponding selected area electron diffraction (SAED) pattern (Fig. 1f) confirmed that the individual nanowire was a single β-Ga_2O_3 crystal with a monoclinic structure (lattice constants $a = 1.223$ nm, $b = 0.304$ nm, $c = 0.580$ nm, and $\beta = 103.7°$ (JCPDS card No. 43-1012)). The dim spots in close proximity to the clear spots indicated that Pt has a monocrystalline fcc structure with a lattice constant of $a = 0.39$ nm (JCPDS No. 04-0802).

The CO gas sensing properties of the β-Ga_2O_3 nanowire sensors and Pt-functionalized Ga_2O_3 nanowire sensors were examined at 100 °C. The curves in Fig. 2a and c show the sensing characteristics of the bare Ga_2O_3 nanowires and Pt-coated Ga_2O_3 nanowires, respectively, to a typical reducing gas, CO (10, 25, 50, and 100 ppm). The resistance decreased upon exposure to CO and was recovered even if it was somewhat lower than the initial value after removing the CO source. The sensor responses were stable and reproducible for repeated testing cycles. Fig. 2b and d shows the enlarged parts of the data of Fig. 2a and b, respectively, which were measured at a CO concentration of 100 ppm for both bare-Ga_2O_3 nanowires and Pt-coated Ga_2O_3 nanowires to identify the moments of gas input and gas stop. The response of the bare-Ga_2O_3 nanowires to CO was slow, whereas the recovery was fast. In contrast, the response was improved greatly by Pt functionalization. The bare Ga_2O_3 nanowires showed responses of 4.2, 4.4, 5.0, 6.6% at CO concentrations of 10, 25, 50, and 100 ppm, respectively (Table 1). In contrast, the Pt-functionalized Ga_2O_3 nanowires showed responses of 115.4, 113.8, 110.9, and 111.7% at CO concentrations of 10, 25, 50, and 100 ppm, respectively (Table 1). Therefore, the responses of the nanowires were improved by 27.8, 26.1, 22.0, and 16.9 fold at CO concentrations of 10, 25, 50 and 100 ppm, respectively.

Table 1 also shows that both the response and recovery times of the nanorod sensor to CO gas were somewhat increased by Pt functionalization, but they were still less than 11 min, which is not too bad for practical use. The response and recovery times of the Pt-functionalized Ga_2O_3 nanorod sensors fabricated in this study are longer than the other reported material nanosensors that showed high responses to CO (Table 2). It is not clear at present why both the response and recovery times of the former are longer

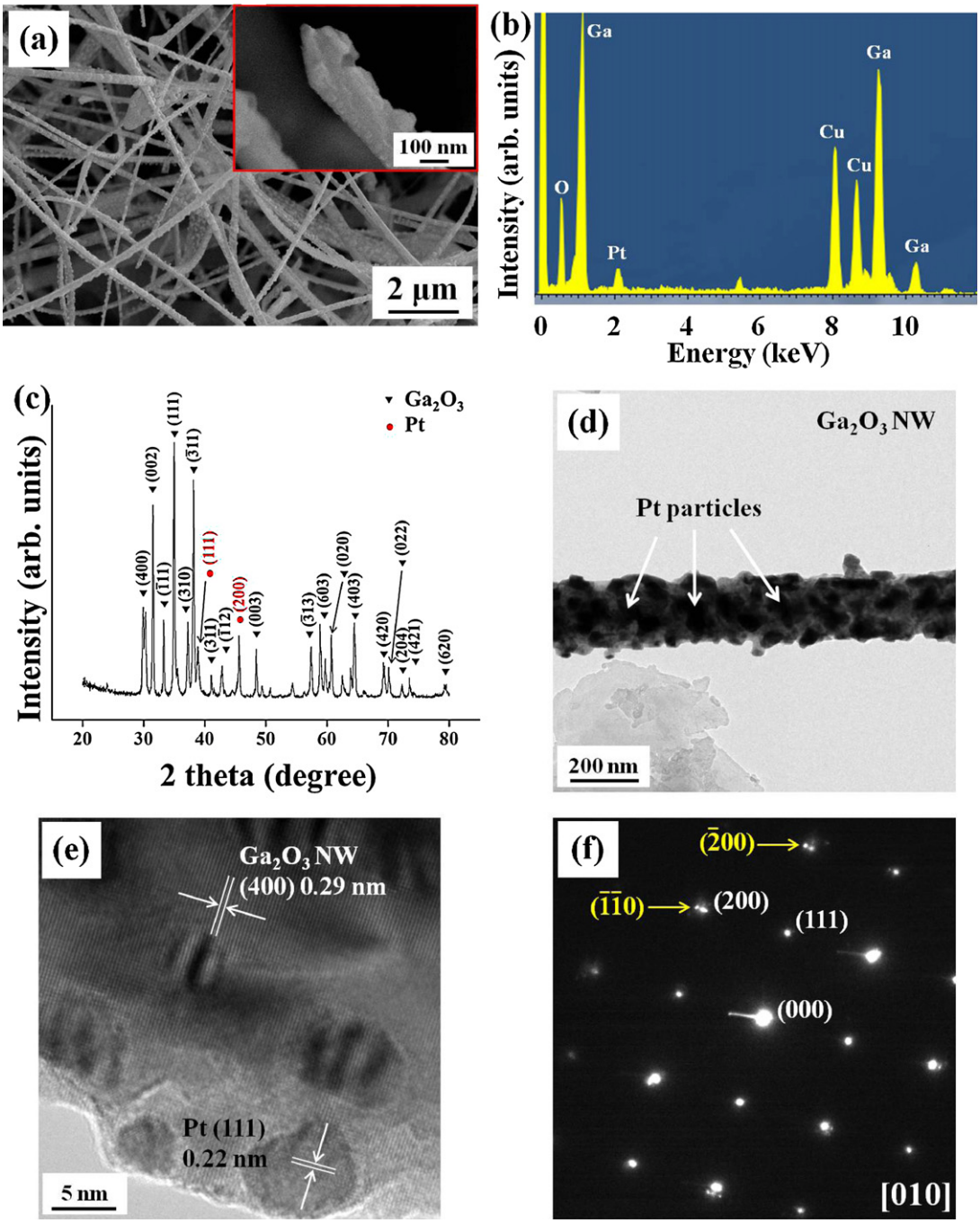

Fig. 1. (a) SEM image of the Pt-coated Ga_2O_3 nanowires. Inset, enlarged SEM image of a typical Pt-coated Ga_2O_3 nanowire. (b) EDX spectrum of the Pt-coated Ga_2O_3 nanowires. (c) XRD pattern of the Pt-coated Ga_2O_3 nanowires. (d) Low-magnification TEM image of a typical of Pt-coated Ga_2O_3 nanowire. (e) Local HRTEM image of the nanostructure at the interface region of a Ga_2O_3-core and a Pt-shell. (f) SAED pattern of the [0 1 0] zone axis of the nanomaterial in the same region as (e).

than those of the latter, but we surmise that it might be due to the slower chemical reaction of Ga_2O_3 with CO than those of other materials with CO. Anyway, the long response and recovery times of Pt-functionalized Ga_2O_3 nanorod sensors still remains a problem to be solved because a shorter response and recovery times are obviously desirable. However, the Pt-functionalized Ga_2O_3 nanorod sensors must be still attractive owing to their higher responses to most other reported material sensors.

Regarding the sensing mechanism of Ga_2O_3 nanowires, the CO gas sensing mechanism of Pt-functionalized Ga_2O_3 nanowires can be explained by previous models proposed for the metal catalyst-enhanced gas sensing of nanomaterials [15,18,19,23–30]. Ga_2O_3 nanowires have a relatively high electrical resistance at low temperatures because Ga_2O_3 is a semiconducting material with a wide energy band gap of 4.9 eV [31]. At high temperatures, reactive oxygen species, such as O^-, O^{2-}, and O_2^-, are chemosorbed to the Ga_2O_3 nanowires, which allow electron transfer. On the other hand, no such chemisorption and electron transfer occur at low temperatures. In the case of Pt-functionalized Ga_2O_3 nanowires, the

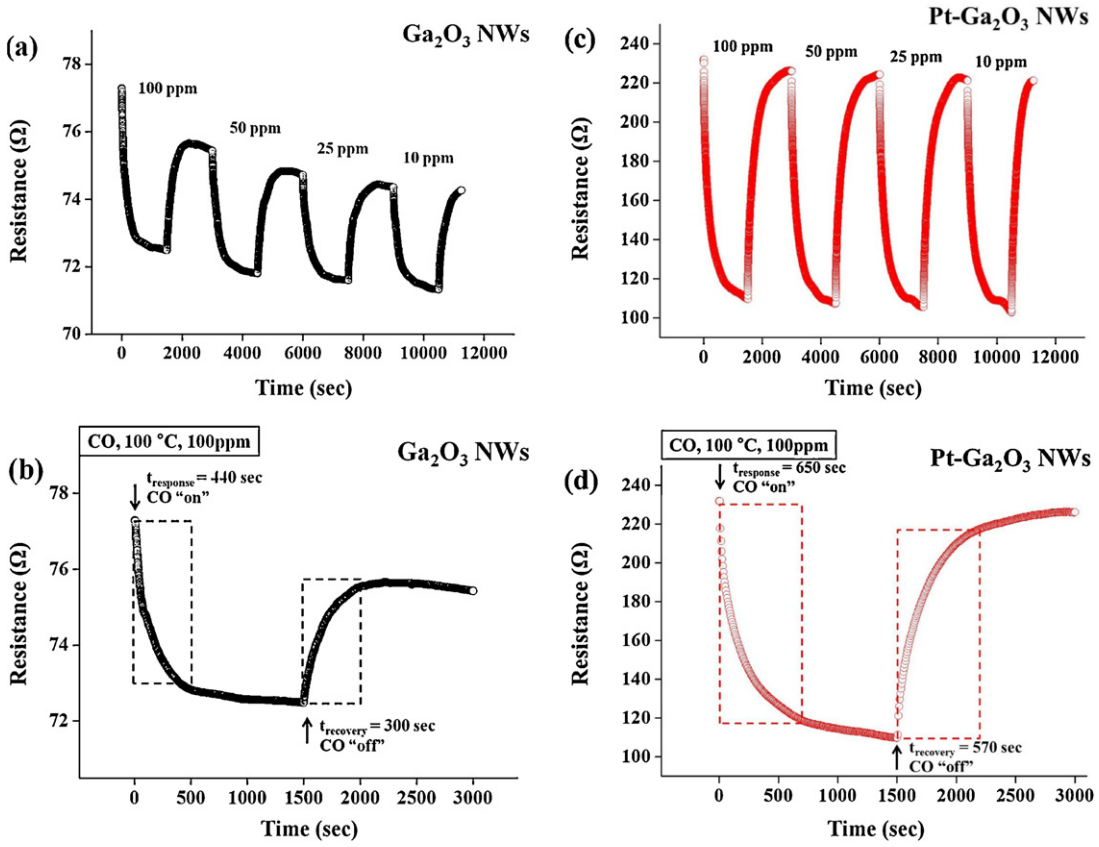

Fig. 2. Electrical response of the gas sensors fabricated from bare and Pt-functionalized Ga_2O_3 nanowires to 10, 25, 50, and 100 ppm CO gas at 100 °C: (a) response curve and (b) enlarged part of the response curve of the bare Ga_2O_3 nanowires-based sensor to 100 ppm CO gas, and (c) response curve and (d) enlarged response curve of the Pt-functionalized Ga_2O_3 nanowire sensor to 100 ppm CO gas.

Table 1
CO gas responses of bare and Pt-functionalized Ga_2O_3 nanowires.

CO conc.	Response (%)		Response time (s)		Recovery time (s)	
	Ga_2O_3	Pt-Ga_2O_3	Ga_2O_3	Pt-Ga_2O_3	Ga_2O_3	Pt-Ga_2O_3
100 ppm	6.61	111.65	440	650	300	570
50 ppm	5.04	110.86	510	600	550	610
25 ppm	4.36	113.76	530	540	430	640
10 ppm	4.15	115.41	560	660	440	400

adsorption of reactive oxygen species is possible, even at low temperatures. The chemisorption of reactive oxygen species occurs on the Pt nanoparticle surface due to the highly conducting nature of Pt. Pt nanoparticles spill oxygen species over the Ga_2O_3 nanowire surface, which is known as the spill-over effect [32,33]. Upon exposure of the Pt-functionalized Ga_2O_3 nanowires to CO gas, CO molecules are adsorbed to the surface of the Pt nanoparticles on the nanowires. The electrons in the conduction band can be trapped by oxygen species, resulting in an electron depletion layer on the of Ga_2O_3 nanowire surface, which increases the resistivity significantly. The adsorbed CO molecules react with preadsorbed oxygen species via the following equations [34]:

$$CO(g) + O^-(ad) \rightarrow CO_2(g) + e^- \quad (1)$$

$$CO + 2O^- \rightarrow {CO_3}^{2-} \rightarrow CO_2 + (1/2)O_2 + 2e^- \quad (2)$$

In the surface sensing reactions, the electrons trapped by the surface oxygen species will be fed back into the electron depletion layer, which will decrease the electrical resistance

Table 2
Comparison of the response and recovery times of nanosensors to CO gas.

Materials	CO conc. (ppm)	T (°C)	Response time (s)	Recovery time (s)	Ref.
Pt-functionalized Ga_2O_3 nanowires	100	100	650	570	Present
Au decorated ZnO nanowire	1000	Room temperature	5	–	[1]
Mesostructured ZnO	20	250	80	90	[2]
ZnO nanowire with the adsorption of Au particles	50	250	40	80	[3]
Nanoflower-like SnO_2	50	275	1.5	30	[4]
Zn-doped In_2O_3 nanowire	5	Room temperature	20	10	[5]
TiO_2 nanofibers	1, 3, 8, 15	200	32–86	84–109	[6]
SnO_2–In_2O_3 nanocomposites	50	50	22 (min)	44 (min)	[7]

of Ga_2O_3. The enhanced chemisorption of oxygen species by the oxygen spillover effect will promote the response of the sensor to the target gases, leading to enhanced sensing properties. Overall, the enhanced electrical response of the Pt-functionalized Ga_2O_3 nanowire sensor to CO gas can be attributed to a combination of the spillover effect as well as the enhanced chemisorption and dissociation of the target gas.

4. Conclusions

The morphology, crystal structure and enhanced sensing characteristics of Pt-functionalized Ga_2O_3 nanostructures to CO gas at 100 °C were investigated. The Ga_2O_3 1D nanostrutures synthesized using an evaporation technique had a wire-like morphology with diameters and lengths ranging from a few tens to a few hundreds of nanometers and up to a few hundreds of micrometers, respectively. The multiple networked gas sensors fabricated from the Ga_2O_3 nanowires functionalized with Pt showed enhanced electrical responses to CO gas at 100 °C. The responses of the nanowires were improved 27.8, 26.1, 22.0, and 16.9 fold at CO concentrations of 10, 25, 50, and 100 ppm, respectively. Both the response and recovery times of the nanowire sensor for CO gas sensing were increased significantly by Pt functionalization, but they were still less than 11 min. A combination of the spillover effect and the enhanced chemisorption and dissociation of the target gas resulted in an increase in the electrical response of the Pt-functionalized Ga_2O_3 nanowire sensor to CO gas.

Acknowledgment

This study was financially supported by the Korean Science and Engineering Foundation (KOSEF) through the 2007 National Research Laboratory (NRL) Program.

References

[1] M. Fleischer, H. Meixner, Selectivity in high-temperature operated semiconductor gas-sensors, Sens. Actuators B 52 (1998) 179–187.
[2] J. Frank, M. Fleischer, H. Meixner, A. Feltz, Enhancement of sensitivity and conductivity of semiconducting Ga_2O_3 gas sensors by doping with SnO_2, Sens. Actuators B 49 (1998) 110–114.
[3] C. Baban, Y. Toyoda, M. Ogita, Oxygen sensing at high temperatures using Ga_2O_3 films, Thin Solid Films 484 (2005) 369–373.
[4] A. Trinchi, W. Wlodarski, Y.X. Li, Hydrogen sensitive Ga_2O_3 Schottky diode sensor based on SiC, Sens. Actuators B 100 (2004) 94–98.
[5] H. Ohta, K. Nomura, H. Hiramatsu, K. Ueda, T. Kamiya, M. Hirano, H. Hosono, Frontier of transparent oxide semiconductors, Solid State Electron. 47 (2003) 2261–2267.
[6] H. Xie, L. Chen, Y. Liu, K. Huang, Preparation and photoluminescence properties of Eu-doped α- and β-Ga_2O_3 phosphors, Solid State Commun. 141 (2007) 12–16.
[7] M. Passlack, N.E.J. Hunt, E.F. Schubert, G.J. Zydzik, M. Hong, J.P. Mannaerts, R.L. Opila, R.J. Fischer, Dielectric-properties of electron-beam deposited Ga_2O_3 films, Appl. Phys. Lett. 64 (1994) 2715–2717.
[8] T. Schwebel, M. Fleischer, H. Meixner, A selective, temperature compensated O_2 sensor based on Ga_2O_3 thin films, Sens. Actuators B 65 (2000) 176–180.
[9] M. Ogita, K. Higo, Y. Nakanishi, Y. Hatanaka, Ga_2O_3 thin film for oxygen sensor at high temperature, Appl. Surf. Sci. 175–176 (2001) 721–725.
[10] Kolmakov, Y. Zhang, G. Cheng, M. Moskovits, Detection of CO and O_2 using tin oxide nanowire sensor, Adv. Mater. 15 (2003) 997–1000.
[11] Y. Liu, E. Koep, M. Liu, A highly sensitive and fast-responding SnO_2 sensor fabricated by combustion chemical vapor deposition, Chem. Mater. 17 (2005) 3997–4000.
[12] M. Law, H. kind, B. Messer, F. Kim, P. Yang, Photochemical sensing of NO_2 with SnO_2 nanoribbon nanosensors at room temperature, Angew. Chem. 114 (2002) 2511–2514.
[13] Y.H. Lin, M.W. Huang, C.K. Liu, J.R. Chen, J.M. Wu, H.C. Shih, The preparation and high photon-sensing properties of fluorinated tin dioxide nanowires, J. Electrochem. Soc. 156 (2009) K196–K199.
[14] N.S. Ramgir, I.S. Mulla, K.P. Vijayamohanan, A room temperature nitric oxide sensor actualized from Ru-doped SnO_2 nanowires, Sens. Actuators B 107 (2005) 708–715.
[15] G. Gundiah, A. Govindaraj, C.N.R. Rao, Nanowires, nanobelts and related nanostructures of Ga_2O_3, Chem. Phys. Lett. 351 (2002) 189–194.
[16] Y.H. Gao, Y. Bando, T. Sato, Y.F. Zhang, X.Q. Gao, Synthesis, Raman scattering and defects of β-GaO nanorods, Appl. Phys. Lett. 81 (2002) 2267–2269.
[17] C.C. Tang, S.S. Fan, M.L. de la Chapelle, P. Li, Silica-assisted catalytic growth of oxide and nitride nanowires, Chem. Phys. Lett. 333 (2001) 12–15.
[18] H.Z. Zhang, Y.C. Kong, Y.Z. Wang, X. Du, Z.G. Bai, J.J. Wang, D.P. Yu, Y. Ding, Q.L. Hang, S.Q. Feng, Ga_2O_3 nanowires prepared by physical evaporation, Solid State Commun. 109 (1999) 677–682.
[19] B.C. Kim, K.T. Sun, K.S. Park, K.J. Im, T. Noh, M.Y. Sung, S. Kim, S. Nahm, Y.N. Choi, S.S. Park, β-GaO nanowires synthesized from milled GaN powders, Appl. Phys. Lett. 80 (2002) 479–481.
[20] M.A. Sanchez-Castillo, C. Couto, W.B. Kim, J.A. Dumestic, Gold-nanotube membranes for the oxidation of CO at gas–water interfaces, Angew. Chem. 116 (2004) 1160–1162.
[21] G. Jágerszki, R.E. Gyurcsányi, L. Höfler, E. Pretsch, Hybridization-modulated ion fluxes through peptide-nucleic-acid-functionalized gold nanotubes. A new approach to quantitative label-free DNA analysis, Nano Lett. 7 (2007) 1609–1612.
[22] Y. Oshima, A. Onga, K. Takayanagi, Helical gold nanotube synthesized at 150 K, Phys. Rev. Lett. 91 (2003) 205503–205506.
[23] K. Ito, T. Ohgami, Hydrogen detection based on coloration of anodic tungsten oxide film, Appl. Phys. Lett. 60 (1992) 938–940.
[24] S. Sekimoto, H. Nakagawa, S. Okazaki, K. Fukuda, S. Asakura, T. Shigemori, S. Takahashi, A fiber-optic evanescent-wave hydrogen gas sensor using palladium-supported tungsten oxide, Sens. Actuators B 66 (2000) 142–145.
[25] S. Okazaki, H. Nakagawa, S. Asakura, Y. Tomiuchi, N. Tsuji, H. Murayama, M. Washiya, Sensing characteristics of an optical fiber sensor for hydrogen leak, Sens. Actuators B 93 (2003) 142–147.
[26] N. Matsuyama, S. Okazaki, H. Nakagawa, H. Sone, K. Fukuda, Response kinetics of a fiber-optic gas sensor using Pt/WO_3 thin film to hydrogen, Thin Solid Films 517 (2009) 4650–4653.
[27] S. Sumida, S. Okazaki, S. Asakura, S. Nakagawa, H. Murayama, T. Hasegawa, Distributed hydrogen determination with fiber-optic sensor, Sens. Actuators B 108 (2005) 508–514.
[28] H. Nakagawa, N. Yamamoto, S. Okazaki, T. Chinzei, S. Asakura, A room-temperature operated hydrogen leak sensor, Sens. Actuators B 93 (2003) 468–474.
[29] H. Shanak, H. Schmitt, J. Nowoczin, C. Ziebert, Effect of Pt-catalyst on gasochromic WO_3 films: optical, electrical and AFM investigations, Solid State Ionics 171 (2004) 99–106.
[30] H.J. Chen, N.S. Xu, S.Z. Deng, D.Y. Lu, Z.L. Li, J. Zhou, J. Chen, Gasochromic effect and relative mechanism of WO_3 nanowire films, Nanotechnology 18 (2007) 205701–205706.
[31] X. Sun, Y. Li, Ga_2O_3 and GaN semiconductor hollow spheres, Angew. Chem. Int. Ed. 43 (2004) 3827–3831.
[32] Y. Shen, T. Yamazaki, Z. Liu, D. Meng, T. Kikuta, Hydrogen sensors made of undoped and Pt-doped SnO_2 nanowires, J. Alloys Compd. 488 (2009) L21–L25.
[33] A.J. Du, S.C. Smith, X.D. Yao, G.Q. Lu, Hydrogen spillover mechanism on a Pd-doped Mg surface as revealed by ab initio density functional calculation, J. Am. Chem. Soc. 129 (2007) 10201–10204.
[34] G. Jimenez-Cadena, J. Riu, F.X. Rius, Gas sensors based on nanostructured materials, Analyst 132 (2007) 1083–1099.